Biosensors and Bioelectronics 48 (2013) 263–269

Contents lists available at SciVerse ScienceDirect

Biosensors and Bioelectronics

journal homepage: www.elsevier.com/locate/bios

Highly sensitive electrochemical lead ion sensor harnessing peptide probe molecules on porous gold electrodes

Wenqiong Su [a,c], MiSuk Cho [a], Jae-Do Nam [b], Woo-Seok Choe [a], Youngkwan Lee [a,*]

[a] School of Chemical Engineering, Sungkyunkwan University, Suwon 440–746, Korea
[b] Department of Polymer Science and Engineering, Sungkyunkwan University, Suwon 440–746, Korea
[c] School of Chemistry and Chemical Engineering, State Key Laboratory of Metal Matrix Composites, Key Laboratory of Thin Film and Microfabrication Technology of the Ministry of Education, Shanghai Jiao Tong University, 800 Dongchuan Road, Shanghai 200240, PR China

ARTICLE INFO

Article history:
Received 14 January 2013
Received in revised form
2 April 2013
Accepted 15 April 2013
Available online 30 April 2013

Keywords:
Lead ion
Peptide
Electrochemical biosensor
Porous gold
Poly(thiophene acetic acid)

ABSTRACT

Lead ion is one of the most hazardous and ubiquitous heavy metal pollutants and poses an increasing threat to the environment and human health. This necessitates rapid and selective detection and/or removal of lead ions from various soil and water resources. Recently, we identified several Pb^{2+} binding peptides via phage display technique coupled with chromatographic biopanning (Nian et al., 2010) where a heptapeptide (TNTLSNN) capable of recognizing Pb^{2+} with high affinity and specificity evolved. In the present study, an electrochemical sensor harnessing this Pb^{2+} affinity peptide as a probe on a porous gold electrode was developed. The three dimensional porous gold electrode was obtained from electrochemical deposition using the dynamic hydrogen bubble template method. A thin layer of poly (thiophene acetic acid) (PTAA) was coated on the porous gold surface. The Pb^{2+} recognizing peptide was immobilized via amide linkage on the PTAA. The developed biosensor was demonstrated to be fast, selective and reproducible in Pb^{2+} detection, exhibiting Pb^{2+}-specific peak current values around −0.15 V in a broad concentration range ($1-1\times10^{7}$ nM) in 10 min despite the repeated use after regeneration.

1. Introduction

Lead has found numerous industrial applications for long time (Nriagu and Pacyna, 1988), giving rise to the occurrence of toxic Pb^{2+} contaminated environment (e.g. wastewater and soil) almost everywhere. Accumulation of Pb^{2+} in human bodies through the food chain and/or inadvertent exposure to the contaminating sources has been implicated in permanent neurological damage, inhibition of fetal development and malfunctioning of many organs including brain (McLachlin et al., 1980; Needleman and Gatsonis, 1990; Aleo et al., 2006).

Therefore, many analytical methods such as inductively coupled plasma mass spectrometry (ICP-MS) (Newman and Georg, 2012), inductively coupled plasma atomic emission spectrometry (ICP-AES) (Badiei et al., 2012), atomic absorption spectrometry (AAS) (Alvarez and Carrillo, 2012) and other physicochemical techniques (Zhao et al., 2012; Willison and Boyer, 2012; Kazemipour et al., 2008; El Zeftawy and Mulligan, 2011) have been developed to monitor metal ions including Pb^{2+} present in various environmental sources. Despite the merits (e.g. a low detection limit and high specificity) of some of these techniques, a majority of these methods rely on expensively sophisticated instruments and also require time-consuming complicated pretreatment of samples and/or operating procedures, often rendering in situ analysis of Pb^{2+} impractical.

In contrast, electrochemical methods have provided relatively simple and low-cost alternatives to realize rapid in situ detection of metal ions without the need for cost-prohibitive specialized equipment. Anodic stripping voltammetry (ASV) (Chen et al., 2012) has been considered as one of the widely used sensitive electrochemical methods for detecting various metal ions including Pb^{2+}. Especially ASV strategies coupled with the use of chemically modified electrodes where target recognizing probes are immobilized provide higher selectivity afforded by probe-mediated preferential capture of specific metal ions of interest (Strutwolf and Williams, 2005). Wang et al., 2012 reported simultaneous detection of Pb^{2+}, Cu^{2+} and Zn^{2+} using a gold macroelectrode modified with Sn film and Au nanoparticles based on a linear correlation between metal ion concentration and ASV peak current value increase from a oxidation potential specific to each ion. Zhang et al., 2011 also developed an electrochemical sensor using Pb^{2+} specific DNAzyme as a probe and layer-by-layer assembled quantum dots as a signal enhancer where ASV peak current was monitored as a signal to detect Pb^{2+} from 1 nM to 1 μM.

The use of metal ion affinity peptides as probes is particularly attractive for development of electrochemical sensors in view of the following merits. Peptides, the simplest biological recognition elements able to capture various metal ions (Yang et al., 2003), allow

* Corresponding author.: Tel.: +82 31 290 7248; fax: +82 31 299 4711.
E-mail address: yklee@skku.edu (Y. Lee).

0956-5663/$ - see front matter © 2013 Elsevier B.V. All rights reserved.
http://dx.doi.org/10.1016/j.bios.2013.04.031

for cost-efficient large scale synthesis, facile modification to facilitate its accommodation into a sensing element and optimization of amino acid sequence or local structure to produce designer peptides with enhanced target recognition ability. Furthermore, peptides possess multidentate binding sites conducive to exhibiting a strong binding affinity to metal ions and allowing the redox active center to remain in close proximity to the transducer for maximum signal output. Despite these merits, only a few examples of using peptide probes for Pb^{2+} detection are found in the literature.

A natural peptide, human angiotensin I, was used for developing an electrochemical sensor (Chow et al., 2005a) to detect Pb^{2+} at a detection limit of 1.9 nM where the reduction peak of cyclic voltammetry (CV) was used as a signal proportional to Pb^{2+} concentration. However, their sensor showed significant cross reactivity with Hg^{2+}. Another Pb^{2+}-binding peptide (DHHTQQHD) (Rica et al., 2010) was used to develop an electrochemical impedance sensor where the Pb^{2+}-binding peptide molecules physisorbed on nanotubes could detect Pb^{2+} as low as 0.01 nM. However, their detection process is quite complicated and required a rather long (i.e. 1 h) incubation time in Pb^{2+} containing sample solution followed by several post-incubation procedures. Besides, selectivity and/or regenerability of the sensor were not reported, posing a limitation for its practical implementation. In the preparation of Pb^{2+} sensor using peptide molecules, designed biosensors should have a high selectivity to Pb^{2+} rather than other metal ions, including transition metal, which is essential for the determination of Pb^{2+}. Our group previously screened a heptapeptide (TNTLSNN) at low pH conditions (3.5–4.5) by a chromatographic biopanning procedure combined with phage display technique (Nian et al., 2010). This peptide showed high specificity and affinity ($K_d = 3.3 \times 10^{-11}$ M) to Pb^{2+} at low pH, providing a promising candidate probe to selectively detect Pb^{2+} in acid solution.

In this study, a novel electrochemical sensor was developed based on a conducting polymer coated nanostructured porous gold electrode with the use of this peptide probe as a recognition element for Pb^{2+}. The three dimensional porous gold electrode was produced through a simple one-step electrochemical deposition (Cherevko and Chung, 2011) and provided a sufficient surface area conducive to fast mass transport of electrons through the electrolyte/electrode interface. A conducting polymer (CP) layer of poly(3-thiophene acetic acid) (PTAA) was next introduced atop the porous gold layer via Au–S bonding to provide intermediate linker molecules to immobilize Pb^{2+} affinity peptide probe by amide linkage formation while allowing the transfer of electrochemical sensing signal (Liaw et al., 1999). During the sensor fabrication process, each modification step was confirmed by cyclic voltammetry (CV), scanning electron microscope (SEM) and X-ray photoelectron spectroscopy (XPS). The performance of thus constructed sensor in Pb^{2+} detection was assessed via ASV based on a peak current value obtained from square wave voltammetry (SWV) curve in view of sensitivity, selectivity and regenerability.

2. Experimental

2.1. Materials and apparatus

3-thiopheneacetic acid (TAA), 4-morpholineethanesulfonic acid (MES), N-hydroxy-succinimide (NHS), N-(3-dimethyl aminopropyl)-N′-ethylcarbodiimide hydrochloride (EDC), ethylene diamine tetraacetic acid (EDTA), anhydrous acetonitrile (ACN) and the nitrate or chloride salts of all the cations (e.g. K^+, Ca^{2+}, Cd^{2+}, Co^{2+}, Cu^{2+}, Mg^{2+}, Ni^{2+}, Zn^{2+}, Cr^{3+} and Fe^{3+}) used in the present study were purchased from Sigmar-Aldrich and used without further purification. Hydorogen tetrachloroaurate (III) hydrate ($HAuCl_4 \cdot Au_2O$, $n=3.6$) was purchased from Kojima Chemicals Co., Ltd. (Japan). Pb^{2+} affinity peptide (TNTLSNN), custom synthesized by Bio-FD&C (Incheon, Republic of Korea), was dissolved in 0.1 M MES buffer (pH 6.8) and stored at 4 °C before use. Bovine serum albumin (BSA, A7906) was purchased from Sigma-Aldrich (St. Louis, MO, USA) and stored at −20 °C until use. Ammonium acetate buffer (50 mM ammonium acetate, 50 mM NaCl, pH 3.5) was used as an electrolyte and also for preparation of varying concentrations of Pb^{2+} analytes. All solutions were freshly prepared using ultrapure water produced by the Sartorious Arium 61316 RO system (Sartorius Stedim Biotech, Aubagne Cedex, France). All the glassware was autoclaved before use. All other chemicals were of analytical grade and used as received.

All the electrochemical experiments were performed using VSP Potentiostat (Princeton applied research, USA) and the data were recorded with VSP EC-Lab software. Cyclic voltammetry (CV) and square wave voltammetry (SWV) were conducted in a conventional three-electrode cell with a gold disc (CH Instruments Inc., USA; diameter: 2 mm), an Ag/AgCl (saturated KCl solution) and a platinum plate as the working, reference and counter electrodes, respectively.

The structures of porous gold and PTAA-coated porous gold electrodes were analyzed by SEM (JSM-7600F, JEOL, Japan) to confirm the morphological changes on the electrode surfaces following electrochemical deposition of porous gold and electrochemical polymerization of PTAA.

X-ray photoelectron spectroscopy (XPS) measurements were carried out using a VG Scientific ESCA 2000 spectrometer (VG Microtech, UK) with an Mg-K^{α} X-ray source set at 170 W (13 mA and 13 kV).

2.2. Fabrication of peptide modified electrode for Pb^{2+} detection

The gold electrodes were polished and cleaned in 30% H_2O_2/98% H_2SO_4 (1/3, v/v) solution for 15 min, rinsed with distilled water, and subjected to electrochemical oxidation by CV between 0 to 1.5 V against the reference electrode at a scan rate of 100 mV/s in 0.5 M H_2SO_4 (Su et al., 2010) until the curves reach a steady state. The electrodes were rinsed with distilled water prior to further modification.

Porous gold electrode was prepared by electrochemical deposition using an aqueous electrolyte comprising 0.01 M $HAuCl_4$ and 2 M NH_4Cl (Cherevko and Chung, 2011). Electrochemical deposition was attempted as varying conditions (i.e. applied potential, deposition time and electrode distance) in order to optimize the morphology of porous gold layers. The CV reduction peak in 0.5 M H_2SO_4 was used to calculate the increased surface area of the electrode following electrochemical deposition of porous gold layers.

After washing and drying, the porous gold electrodes were immersed in 0.1 M $LiClO_4$/ACN solution containing 0.1 M TAA (degassed by nitrogen before use). A constant potential of 1.5 V was applied for 15 s at room temperature (Pardieu et al., 2009). The PTAA/porous gold electrodes thus prepared were incubated in 100 mM MES buffer containing 20 mM EDC and 20 mM NHS to introduce activated carboxyl groups to PTAA for 15 min. Following rinsing with MES buffer, the electrodes were transferred to 100 mM MES buffer containing 0.25 mg/ml of Pb^{2+} affinity peptide and incubated for 1 h to render covalent binding of the peptide to PTAA (Su et al., 2012). The peptide modified electrode was rinsed thoroughly with MES buffer and further blocked in 1% BSA/PBS (10 mM, pH 7.4) solution for 1 h. The peptide modified electrode was stored at 4 °C in ammonium acetate buffer prior to use. A schematic diagram of the stepwise procedure of the peptide modified electrode was shown in Fig. 1.

2.3. Performance of peptide modified electrode on Pb^{2+}detection

$Pb(NO_3)_2$ was dissolved in ammonium acetate buffer to give a 10 mM Pb^{2+} stock solution. The standard solutions with different concentrations of Pb^{2+} (1 nM, 10 nM, 100 nM, 1 μM, 10 μM, 100 μM,

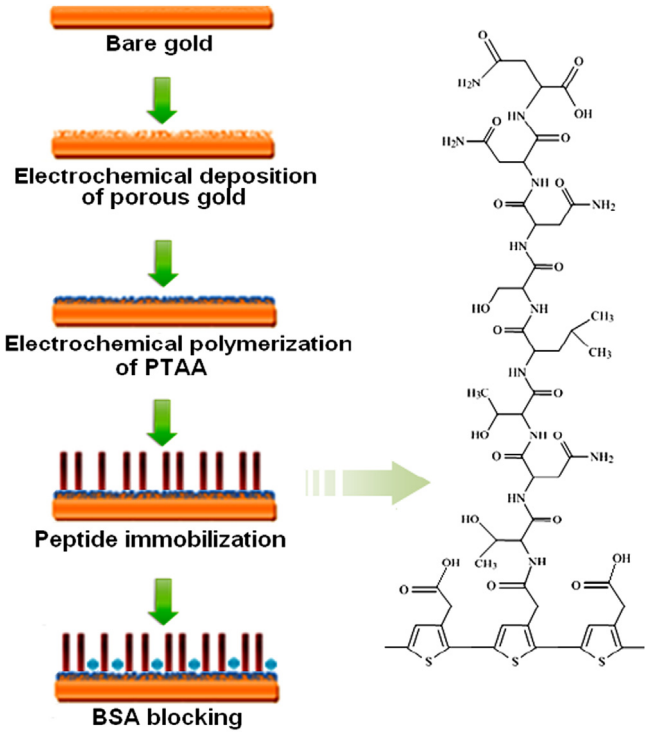

Fig. 1. A schematic of the stepwise procedure for fabricating the peptide modified electrode.

and 1 mM) were prepared by successively diluting the stock solution. The peptide-modified electrode was immersed in each Pb^{2+} standard solution for 10 min and washed with Pb^{2+}-free ammonium acetate buffer. The Pb^{2+} captured on the peptide-modified electrode surface were reduced at −1.1 V for 1 min followed by SWV measurement of the electrochemical response from −0.5 to 0.5 V at a frequency of 25 Hz, an amplitude of 25 mV, a step voltage of 4 mV and a static time of 30 s.

Following electrochemical detection of Pb^{2+}, the used electrode was regenerated by rinsing with 1 mM EDTA solution for 1 min, incubated in ammonium acetate buffer for 5 min, and further thoroughly rinsed with ammonium acetate buffer. The regenerated electrode was placed in ammonium acetate buffer lacking Pb^{2+} and reduced prior to confirming efficient stripping of Pb^{2+} from the electrode by SWV measurement. In order to investigate the specificity of the peptide probe towards Pb^{2+}, the sensor performance was assessed against acetate buffer containing 50 μM of various cations (e.g. K^+, Ca^{2+}, Cd^{2+}, Co^{2+},Cu^{2+}, Mg^{2+}, Ni^{2+}, Zn^{2+}, Cr^{3+} and Fe^{3+}) which may potentially exhibit cross binding reactivity to the Pb^{2+} affinity peptide.

3. Results and discussion

3.1. Preparation of peptide modified electrode

The porous gold layer was electrochemically deposited directly on the working electrode surface by dynamic hydrogen bubble template method in 10 mM $HAuCl_4$ aqueous solution containing 2 M NH_4Cl. The deposition conditions were optimized in conjunction with the applied voltage (−3, −4 and −5 V), the deposition time (10, 20 and 30 s) and the distance between working and counter electrode (0.5, 1 and 1.5 cm). The deposition time and voltage are the essential factors to govern the structural property of electrochemically deposited porous gold layers. The voltage at the time of electrodeposition determines the reaction rate which in turn affects the speed of releasing hydrogen bubbles. The amount of porous gold or the thickness of porous gold layer is proportional to the duration of electrodeposition. Besides, the distance between working and counter electrode is also a critical factor to affect the morphology of the deposited porous gold layer. This is because the inter-electrodic space determines a mean travel distance of hydrogen bubbles along which the bubbles inflate to larger sizes, thereby exerting direct impact on the porosity of the deposited gold layer.

The morphology of electrochemically deposited porous gold layers was investigated by SEM. Fig. 2A and B showed the porous gold layer obtained under the optimized condition (i.e. −4 V, 20 s and 1 cm). It is noted that the porous gold layer formed at this condition reveals a three dimensional dendrite network nanostructure conducive to provide large surface area mediated fast electron transfer, potentially useful for fabricating electrochemical sensors with enhanced sensitivity.

The PTAA was subsequently coated on the porous gold surface via electrochemical deposition at 1.5 V for 15 s. The thickness and morphology of PTAA layer plays an important role in determining a sensor performance. An excess amount of PTAA hence the formation of highly crowded PTAA layer would efface the microstructure of porous gold despite offering abundant active sites to immobilize peptide probe molecules. Fig. 2C and D showed the morphology of PTAA-covered porous gold electrode whose surface was uniformly covered by a thin layer of PTAA conducting film.

The porous gold electrode was electrochemically characterized by CV in 0.5 M H_2SO_4 at a scan rate of 100 mV/s (Fig. 3A, curve *b*). Compared with the CV curve of bare gold electrode (Fig. 3A, curve *a*), the reduction peak of the porous gold electrode was found to be much larger, indicative of the significantly enhanced electrode surface area due to the presence of porous nanostructure (Hu et al., 2008). The gold oxide formed in the positive sweep was then electrochemically reduced in the negative potential sweep. Under the same electrochemical conditions, an effective surface area is in proportion to the charge required for reducing the gold oxide (Chen et al., 2008). By integrating the reduction peak areas of bare and porous gold electrodes, the effective area was calculated to be approximately 155 times increased after the electrochemical deposition of the porous gold layer.

Following electrochemical deposition of PTAA on porous gold surface, the stability of the conducting polymer film was investigated by *CV* in ammonium acetate buffer in the potential range of −0.6 to 1.4 V at a scan rate of 100 mV/s. During the 10 repetitive potential cycles (Fig. 3B), the reversible redox system showed a reduction peak at 0.65 V and an oxidation peak at 1.25 V consistently, which is in good agreement with those reported elsewhere (Visy et al., 2000). The presence of reproducible redox peaks indicates the formation of a stable conducting PTAA film to facilitate accommodation of the peptide probes in the latter stage. Moreover Fig. 3B (inset) showed the SWV curves obtained from PTAA/porous gold electrodes in the presence or absence of Pb^{2+} and with or without the peptide probe molecules coupled under variation of the applied potential between −0.5 and 0.5 V in ammonium acetate buffer. The PTAA/porous gold electrode presented a flat curve in ammonium acetate buffer lacking Pb^{2+} for the potential range explored (Fig. 3B, curve *c* (inset)). Following immobilization of the Pb^{2+} affinity peptide and blocking of BSA onto the PTAA layer, the SWV responses for the peptide modified electrode in the presence (Fig. 3B, curve *a* (inset)) and absence (Fig. 3B, curve *b* (inset)) of 1 nM Pb^{2+} were compared. A distinctive peak at −0.15 V (Fig. 3B, curve *a* (inset)) appeared from the peptide modified electrode upon its incubation with Pb^{2+}, accounting for peptide-mediated Pb^{2+} capture followed by oxidation of the reduced lead at −1.1 V from the electrode surface. Based on this observation, a peak current observed atop the SWV peak at −0.15 V was used as a sensing signal for Pb^{2+} detection with the developed sensors.

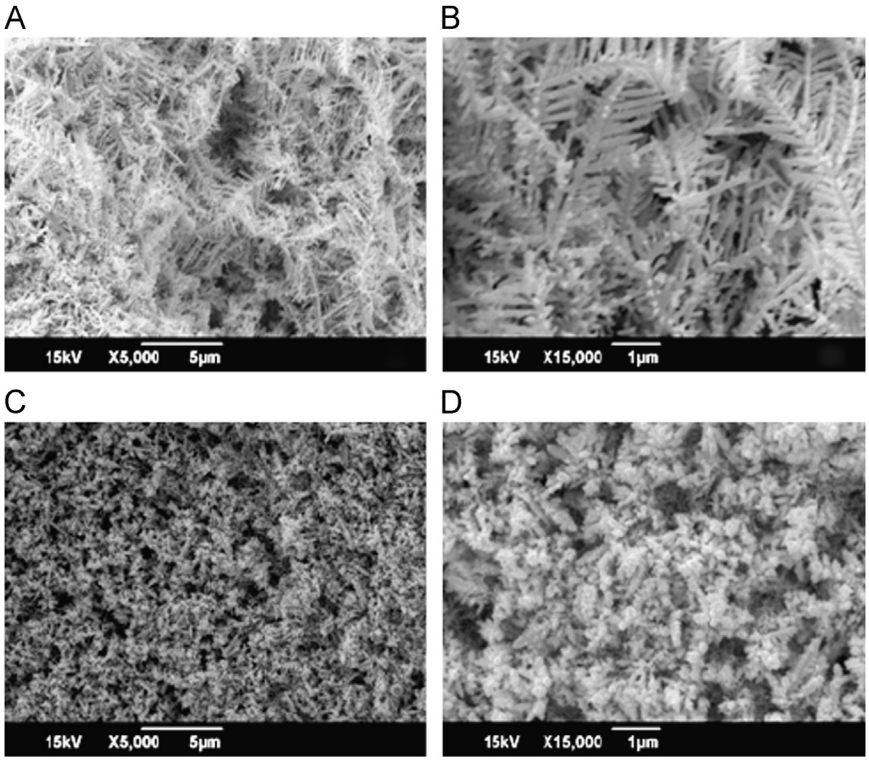

Fig. 2. SEM images of porous gold (A and B) and PTAA-covered porous gold (C and D) layers at different magnifications.

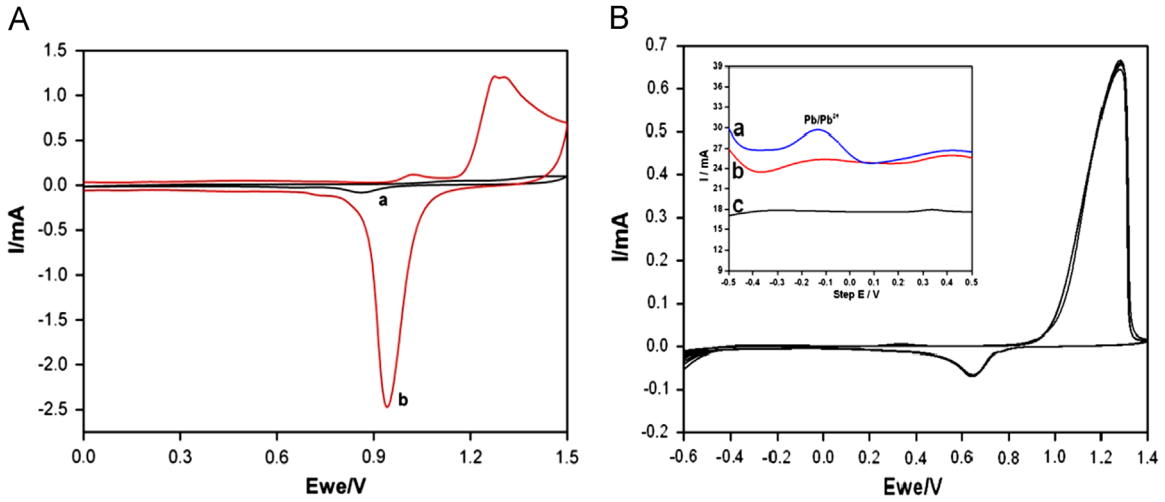

Fig. 3. Electrochemical analysis of various electrodes fabricated in the present study: (A) CV curves obtained from bare (a) and porous gold (b) electrodes in 0.5 M H_2SO_4 from 0 to 1.5 V at a scan rate of 100 mV/s; (B) CV curves for PTAA/porous gold electrode in ammonium acetate buffer from −0.6 to 1.4 V at a scan rate of 100 mV/s for 10 cycles (inset: SWV curves obtained from BSA/peptide/PTAA/porous gold electrode after incubation in ammonium acetate buffer containing Pb^{2+} (a), BSA/peptide/PTAA/porous gold electrode in Pb^{2+}-free ammonium acetate buffer (b) and PTAA/porous gold electrode in Pb^{2+}-free ammonium acetate buffer (c) for a voltage range from −0.5 to 0.5 V).

Fig. 4 showed the XPS data after immobilizing the Pb^{2+} binding peptide molecules on the PTAA covered porous gold surface. The amino groups of the amino acid residues in the peptide were reacted with the carboxylic acid groups of PTAA film (Kim et al., 2008), giving rise to amido bonds to covalently anchor the peptide probes on the substrate. The S_{2p} spectrum of PTAA modified electrode (Fig. 4A) is fitted to give two peaks. The peak at 161.8 eV can be attributed to S–Au (Gamero et al., 2012), accounting for the presence of thiophene rings attached to the gold surface with carboxylic acid groups outwardly exposed. The peak at 165.4 eV comes from S–C of the PTAA molecules, in good agreement with the peak position reported by Khan et al. (2000). The N_{1s} spectrum of peptide modified electrode (Fig. 4B) revealed two peaks, one at 398.1 eV (–NH_2–) and the other at 399.9 eV (–NH–) in association with the presence of peptide molecules, whose locations corresponded well with those reported elsewhere (Kannan and John, 2011). After immobilization of peptide molecules, the unreacted carboxylic acid groups of PTAA were further passivated by the use of BSA as a blocking agent in order to minimize nonspecific binding of any interfering species to the probe. For the peptide modified electrode placed in ammonium acetate buffer containing 1 nM Pb^{2+} for 10 min, the Pb 4f XPS spectra (Fig. 4C) showed two peaks at 138.4 eV and 143.5 eV (Zhao et al., 2007) arising from the presence of Pb^{2+} captured by the peptide probe on the electrode surface.

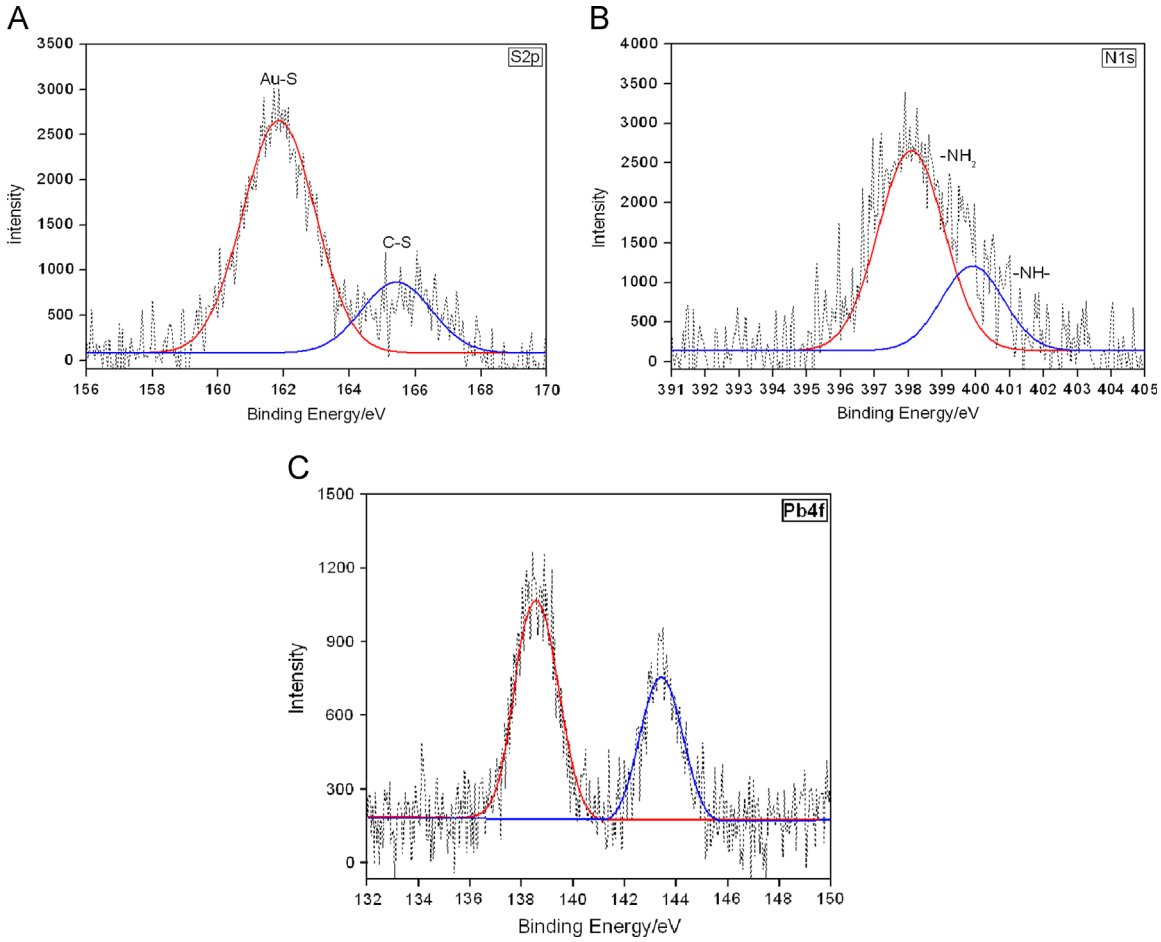

Fig. 4. XPS analysis for (A) PTAA/porous gold electrode, (B) peptide/PTAA/ porous gold electrode and (C) Pb^{2+}-loaded BSA/peptide/PTAA/ porous gold electrode.

3.2. *Performance of the electrochemical sensor on Pb^{2+} detection*

The extent of specific interaction between Pb^{2+} and its affinity peptide probe immobilized on the electrode can be directly quantified by monitoring an electrochemical signal whose change is proportional to the amount of Pb^{2+} in solution. As discussed early (Fig. 3B (inset)), the electrochemical sensor based on peptide modified electrode showed a distinctive peak current value atop SWV response curve for a small amount of Pb^{2+} following incubation in 1 nM Pb^{2+} solution. In order to explore a dynamic detection range of the developed senor in detecting Pb^{2+}, the electrode was incubated in acetate buffer containing varying concentrations of Pb^{2+}, reduced at −1.1 V and subsequently subjected to SWV analysis as shown in Fig. 5A. It was found that the peak current change (i.e. ΔI) showed a good linear relationship ($\Delta I = 7.84 \times \log([Pb^{2+}/\mu M]) + 27.75$ with R^2 value of 0.994) with Pb^{2+} concentration from 1 nM to 10 mM (Fig. 5 B). It is well known that pH condition significantly affects the solubility of Pb^{2+} and that $Pb(OH)_2$ is formed and precipitated even at pH 5 (Nian et al., 2010). It would therefore be impractical to measure Pb^{2+} concentration around neutral pH conditions. Furthermore, the efficiency of probe-target interaction is often affected by pH condition too. For examples, proteins (Guo et al., 2011) and nucleic acids (Su et al., 2012) probes have usually been used at physiological conditions and would otherwise lose their target recognition ability. On the other hand, the screening of Pb^{2+} affinity peptide used as a probe in this study was conducted at acidic conditions (i.e. pH 3.5–4.5) via chromatographic biopanning with the use of phage displayed peptide library (Nian et al., 2010). This rendered electrochemical determination of Pb^{2+} realized at a relatively low pH of 3.5 where most of Pb^{2+} is stable.

The performance of our Pb^{2+} sensor was also assessed in detecting Pb^{2+} in a real sample obtained from Han River which runs through the downtown of Seoul. After adjusting the pH value to 3.5, the Pb^{2+} concentration in the water sample was estimated to be 7.0 ± 0.5 nM by the developed sensor, comparable to that (i.e. 6.0 ± 0.1 nM) determined by ICP-MS (Agilent 7500, Agilent Technologies Inc.) measurement.

3.3. *Selectivity and regenerability of the Pb^{2+} electrochemical sensor*

The performance of the electrochemical sensor in selective recognition of Pb^{2+} was investigated in the presence of various interfering species (i.e. Cu^{2+}, Ni^{2+}, Mg^{2+}, Cd^{2+}, Co^{2+}, Ca^{2+}, K^{+}, Zn^{2+}, Fe^{3+} and Cr^{3+}) reported to frequently co-exist with Pb^{2+} (Badiei et al., 2012; Cherevko and Chung, 2011). As shown in Fig. 6A, the peptide modified gold electrode showed preferential high affinity to Pb^{2+} with negligible cross reactivity exhibited towards all the above-listed interferents despite the presence of a large excess amount of these interfering metal ions (i.e. 50 μM) as compared to that of the target analyte Pb^{2+} (i.e. 1 nM).

The underpinning mechanism to explain this highly selective recognition of Pb^{2+} by the peptide probe (TNTLSNN) used in this study is not clear. However, it is interesting to note that our peptide probe has no histidines (Chow et al., 2005b) and glutathiones (Bontidean et al., 2003; Beqa et al., 2011) residue frequently encountered in many affinity peptides reported to have strong affinity towards heavy and/or transition metal ions at neutral pH conditions. This is possibly because our Pb^{2+} affinity peptide was screened at a low pH condition where a protonated form of these amino acids less

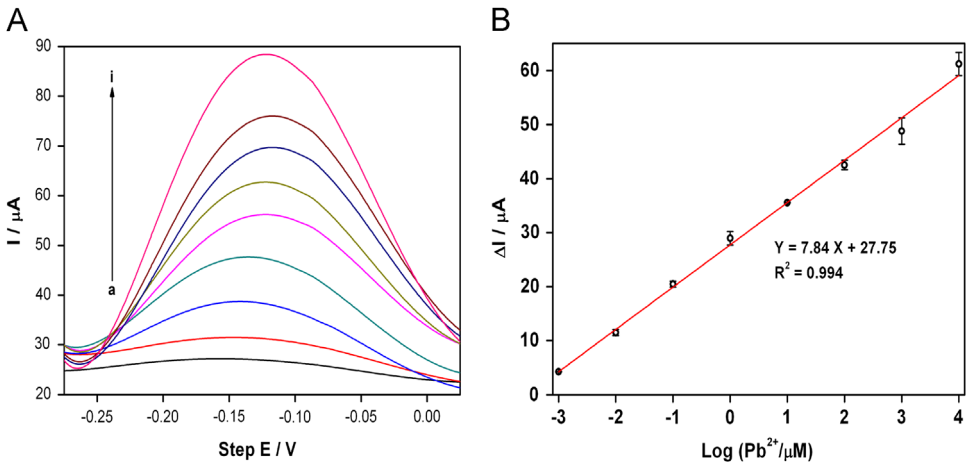

Fig. 5. Assessment of the performance of the peptide modified electrode on Pb^{2+} detection. (A) SWV curve profiles (zoomed in after voltage excursion from −0.5 to 0.5 V) where peak current values increase with Pb^{2+} concentration from 1 nM to 10 mM (curve *a*: baseline (i.e. acetate buffer lacking Pb^{2+}); curves *b* to *i*: 1 nM to 10 mM of Pb^{2+} in ammonium acetate buffer). (B) The calibration curve fit to show a linear relationship between SWV peak current and Pb^{2+} concentration.

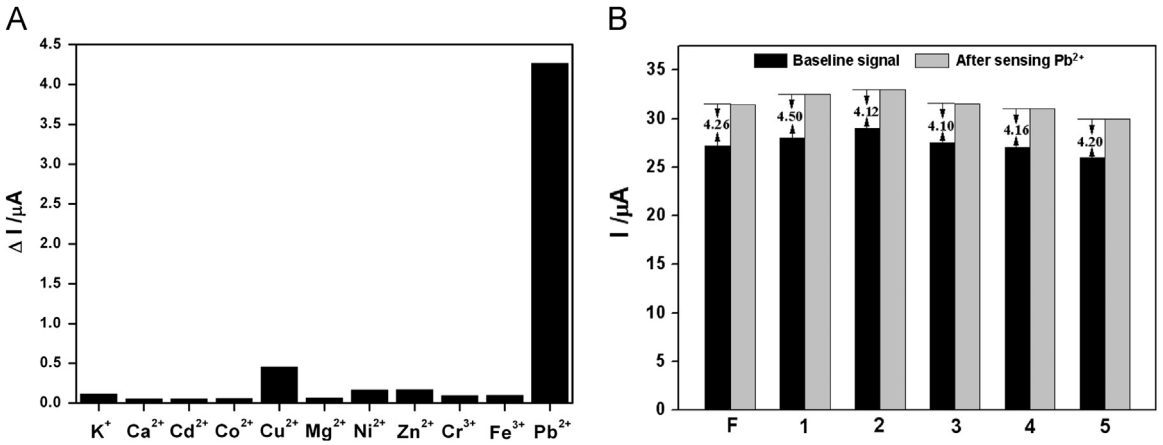

Fig. 6. (A)The peak current changes (ΔI) atop SWV signal response curves obtained from the peptide modified electrode incubated in ammonium acetate buffer containing 1 nM of Pb^{2+} or 50 μM of various other metal ions. (B) Assessment of the sensor performance in Pb^{2+} detection during 5 times of regeneration cycle. The peak current value changes in the repeated SWV analyses for fresh and regenerated electrode incubated in ammonium acetate buffer containing 1 nM Pb^{2+} are shown (F: fresh sensor; 1–5: reused sensor after each regeneration cycle with EDTA).

conducive to metal ion biding is dominant. Instead our peptide probe is highly enriched with polar but uncharged amino acid residue (i.e. 3 asparagine (N)) and hydroxyl amino acid residues (2 threonine (T) and 1 serine (S)). This unusual amino acid sequence pattern of the Pb^{2+} probe peptide may partially account for its highly specific Pb^{2+} recognition ability and/or negligible cross binding affinity to various other metal ions.

The performance of the electrochemical sensor was also evaluated following regeneration of the used sensor with 1 mM EDTA according to the procedure described in Section 2.3. Upon detection of 1 nM Pb^{2+} in acetate buffer with a fresh peptide modified electrode, the same electrode was subjected to 5 times of regeneration cycle. Between each cycle, the regenerated electrode was placed in ammonium acetate buffer containing 1 nM Pb^{2+} prior to taking a peak current reading from each SWV analysis. The results summarized in Fig. 6B show that the regenerated electrode retained its reactivity to Pb^{2+}, giving rise to reproducible peak current readings from SWV analysis in the repeated measurement quite close to that of the fresh electrode with a relative standard deviation of 3.5%. This clearly indicates that our electrochemical sensor could be regenerated by a simple EDTA based regeneration protocol at least 5 times without compromising its Pb^{2+} sensing ability. For comparison purposes, we summarize some recent reports using different recognition elements and approaches for Pb^{2+} sensing in Supplemental information.

4. Conclusions

In this study, a successful fabrication of a Pb^{2+} detecting electrochemical biosensor harnessing highly specific Pb^{2+} affinity peptide probe immobilized on porous gold electrode was demonstrated. The developed biosensor showed a good sensitivity of detecting as low as 1 nM of Pb^{2+} in low pH condition with a broad linear dynamic detection range between 1 nM and 10 mM. In addition, the demonstrated electrochemical sensor was very specific in selectively capturing Pb^{2+} without exhibiting cross reactivity towards various metal ions often found to interfere with Pb^{2+} detection. Finally, our sensor could be regenerated to give an uncompromised Pb^{2+} sensing ability by a simple regeneration protocol using a low concentration of EDTA. Taken together, the demonstrated strategy to construct an electrochemical sensor platform using a target-specific affinity probe immobilized on large surface porous nanostructured electrode is expected to provide a number of advantages such as low-cost, short detection time and facile operation, thereby showing a good potential to broaden its practical application.

Acknowledgment

This research was supported by Basic Science Research Program through the National Research Foundation of Korea (NRF) funded by the Ministry of Education, Science and Technology (2009-0083540) and (R1A2A2A01-2010-0014165).

Appendix A. Supporting information

Supplementary data associated with this article can be found in the online version at http://dx.doi.org/10.1016/j.bios.2013.04.031.

References

Aleo, M.F., Bettoni, F., Boniotti, J., Morandini, F., Giuliani, R., Steimberg, N., Apostoli, P., Mazzoleni, G., 2006. Toxicology in Vitro 20, 874–881.
Alvarez, M.A., Carrillo, G., 2012. Talanta 97, 505–512.
Badiei, H.R., Liu, C., Karanassios, V., 2012. Microchemical Journal , http://dx.doi.org/10.1016/j.microc.2 012.10.013.
Beqa, L., Singh, A.K., Khan, S.A., Senapati, D., Arumugam, S.R., Ray, P.C., 2011. ACS Applied Materials & Interfaces 3, 668–673.
Bontidean, I., Ahlqvist, J., Mulchandani, A., Chen, W., Bae, W., Mehra, R.K., Mortari, A., Csoregi, E., 2003. Biosensors and Bioelectronics 18, 547–553.
Chen, L., Su, Z.H., He, X.H., Liu, Y., Qin, C., Zhou, Y.P., Li, Z., Wang, L.H., Xie, Q.J., Yao, S.Z., 2012. Electrochemistry Communications 15, 34–37.
Chen, X., Wang, Y., Zhou, J., Yan, W., Li, X., Zhu, J.J., 2008. Analytical Chemistry 80, 2133–2140.
Cherevko, S., Chung, C.H., 2011. Electrochemistry Communications 13, 16–19.
Chow, E., Hibbert, D.B., Gooding, J.J., 2005a. Analytica Chimica Acta 543, 167–176.
Chow, E., Wong, E.L.S., Bocking, T., Nguyen, Q.T., Hibbert, D.B., Gooding, J.J., 2005b. Sensors and Actuators B: Chemical 111–112, 540–548.
El Zeftawy, M.A.M., Mulligan, C.N., 2011. Separation and Purification Technology 77, 120–127.
Gamero, M., Fierro, J.L.G., Lorenzo, E., Alonso, C., 2012. Electroanal 24, 1–10.
Guo, Y., Wang, Z., Qu, W., Shao, H., Jiang, X., 2011. Biosensors and Bioelectronics 26, 4064–4069.
Hu, K., Lan, D., Li, X., Zhang, S., 2008. Analytical Chemistry 80, 9124–9130.
Kannan, P., John, S.A., 2011. Electrochimica Acta 56, 7029–7037.
Kazemipour, M., Ansari, M., Tajrobehkar, S., Majdzadeh, M., Kermani, H.R., 2008. Journal of Hazardous Materials 150, 322–327.
Khan, M.A., Armes, S.P., Perruchot, C., Ouamara, H., Chehimi, M.M., Greaves, S.J., Watts, J.F., 2000. Langmuir 16, 4171–4179.
Kim, H.J., Lee, K.S., Won, M.S., Shim, Y.B., 2008. Langmuir 24, 1087–1093.
Liaw, D.J., Liaw, B.Y., Gong, J.P., Osada, Y., 1999. Synthetic Metals 99, 53–59.
McLachlin, J.R., Goyer, R.A., Cherian, M.G., 1980. Toxicology and Applied Pharmacology 56, 418–431.
Needleman, H.L., Gatsonis, C.A., 1990. JAMA 263, 673–678.
Newman, K., Georg, R.B., 2012. Chemical Geology 304-305, 151–157.
Nian, R., Kim, D.S., Nguyen, T., Tan, L., Kim, C.W., Yoo, I.K., Choe, W.S., 2010. Journal of Chromatography A 1217, 5940–5949.
Nriagu, J.O., Pacyna, J.M., 1988. Nature 333, 134–139.
Pardieu, E., Cheap, H., Vedrine, C., Lazerges, M., Lattach, Y., Garnier, F., Remita, S., Pernelle, C., 2009. Analytica Chimica Acta 649, 236–245.
Rica, R., Mendoza, E., Matsui, H., 2010. Small 6, 1753–1756.
Strutwolf, J., Williams, D.E., 2005. Electroanal 17, 1970–1976.
Su, W., Nguyen, H.T., Cho, M., Son, Y., Lee, Y., 2010. Synthetic Metals 160, 2471–2475.
Su, W., Lin, M., Lee, H., Cho, M., Choe, W.S., Lee, Y., 2012. Biosensors and Bioelectronics 32, 32–36.
Visy, C., Kankare, J., Krivan, E., 2000. Electrochimica Acta 45, 3851–3864.
Wang, J., Bian, C., Tong, J., Sun, J., Xia, S., 2012. Electroanal 24, 1783–1790.
Willison, H., Boyer, T.H., 2012. Water Research 46, 2385–2394.
Yang, W., Chow, E., Willett, G.D., Hibbert, D.B., Gooding, J.J., 2003. Analyst 128, 712–718.
Zhang, H., Jiang, B., Xiang, Y., Su, J., Chai, Y., Yuan, Y., 2011. Biosensors and Bioelectronics 28, 135–138.
Zhao, L., Zhong, S., Fang, K., Qian, Z., Chen, J., 2012. Journal of Hazardous Materials 239–240, 206–212.
Zhao, W., Ge, P.Y., Xu, J.J., Chen, H.Y., 2007. Langmuir 23, 8597–8601.